

The effect of Ga vacancies on the defect and magnetic properties of Mn-doped GaN

Joongoo Kang and K. J. Chang

Citation: *J. Appl. Phys.* **102**, 083910 (2007); doi: 10.1063/1.2799962

View online: <http://dx.doi.org/10.1063/1.2799962>

View Table of Contents: <http://jap.aip.org/resource/1/JAPIAU/v102/i8>

Published by the [American Institute of Physics](#).

Additional information on J. Appl. Phys.

Journal Homepage: <http://jap.aip.org/>

Journal Information: http://jap.aip.org/about/about_the_journal

Top downloads: http://jap.aip.org/features/most_downloaded

Information for Authors: <http://jap.aip.org/authors>

ADVERTISEMENT



AIP Advances

Now Indexed in Thomson Reuters Databases

Explore AIP's open access journal:

- Rapid publication
- Article-level metrics
- Post-publication rating and commenting

The effect of Ga vacancies on the defect and magnetic properties of Mn-doped GaN

Joongoo Kang

Department of Physics, Korea Advanced Institute of Science and Technology, Daejeon 305-701, Korea

K. J. Chang^{a)}

Department of Physics, Korea Advanced Institute of Science and Technology, Daejeon 305-701, Korea and Korea Institute for Advanced Study, Seoul 130-722, Korea

(Received 27 June 2007; accepted 29 August 2007; published online 24 October 2007)

We perform first-principles theoretical calculations to investigate the effect of the presence of Ga vacancy on the defect and magnetic properties of Mn-doped GaN. When a Ga vacancy (V_{Ga}) is introduced to the Mn ions occupying the Ga lattice sites, a charge transfer occurs from the Mn d band to the acceptor levels of V_{Ga} , and strong Mn–N bonds are formed between the Mn ion and the N atoms in the neighborhood of V_{Ga} . The charge transfer and chemical bonding effects significantly affect the defect and magnetic properties of Mn-doped GaN. In a Mn- V_{Ga} complex, which consists of a Ga vacancy and one Mn ion, the dangling bond orbital of the N atom involved in the Mn–N bond is electrically deactivated, and the remaining dangling bond orbitals of V_{Ga} lead to the shallowness of the defect level. When a Ga vacancy forms a complex with two Mn ions located at a distance of about 6 Å, which corresponds to the percolation length in determining the Curie temperature in diluted Mn-doped GaN, the Mn d band is broadened and the density of states at the Fermi level is reduced due to two strong Mn–N bonds. Although the broadening and depopulation of the Mn d band weaken the ferromagnetic stability between the Mn ions, the ferromagnetism is still maintained because of the lack of antiferromagnetic superexchange interactions at the percolation length. © 2007 American Institute of Physics. [DOI: 10.1063/1.2799962]

I. INTRODUCTION

Since Mn-doped GaN was theoretically predicted to be ferromagnetic above room temperature,¹ this material has attracted considerable attention due to potential applications for spintronic devices, combined with existing technologies in nitride-based photonics and electronic devices. However, experiments so far are quite controversial, reporting the ferromagnetic, antiferromagnetic, and spin-glass phases.^{2–8} Since the Mn ion in GaN has a deeper acceptor level than that of GaAs,^{9–11} the carrier-mediated exchange interaction is inappropriate in explaining the ferromagnetism of Mn-doped GaN.¹² As an alternative mechanism, the d – d direct exchange interaction, the so-called double exchange, was proposed.^{13,14} Since this mechanism is mediated by the localized holes of the Mn ions, the ferromagnetic stability depends on the population of the Mn d band. It was shown that magnetic exchange interactions, which are dominated by the double-exchange mechanism, are short ranged.¹⁵ Thus, unless Mn concentrations are high, it is difficult to achieve the magnetic percolation, leading to low Curie temperatures.^{15,16} Very recently, it was suggested that the nanoscale spinodal decomposition, which produces strong concentration fluctuations, is responsible for high Curie temperatures often observed in wide-gap dilute magnetic semiconductors.^{17–20}

Generally, transition metal ions have low solubilities in III–V semiconductors.²¹ Thus, nonequilibrium growth techniques are often used to introduce transition metal ions into

the host material beyond the solubility limits.^{5,21,22} In such growth processes, a large concentration of intrinsic defects is generated, so that these defects will significantly affect the electronic and magnetic properties by interacting with transition metal ions. For example, the generation of Ga vacancies (V_{Ga}) is highly expected in Mn-doped GaN epitaxially grown at low temperatures under N-rich conditions,²³ where the Mn ions beyond the solubility limit are incorporated. To tune the electrical and magnetic properties of GaMnN for specific device applications, it is imperative to understand the details of interactions between the Mn-doped host material and intrinsic defects. In recent calculations by Mahadevan and co-workers,²⁴ the role of V_{Ga} was studied in modifying the magnetic interactions between two Mn ions at the nearest-neighbor distance, and a depopulation of the Mn d band was found to reduce the exchange splitting of the Mn band and hence destroy the ferromagnetism. In diluted Mn-doped GaN, since the distances between the Mn ions will be larger than the nearest-neighbor distance, it is more appropriate to consider the Mn ions separated by the percolation length of about 6 Å,²⁵ which is employed to determine the Curie temperature.

In this paper, we investigate interactions of a Ga vacancy with the Mn ions in Mn-doped GaN and their influence on the defect and magnetic properties through density functional calculations in the generalized-gradient approximation (GGA) as well as within the GGA+ U approach. We find that introducing a Ga vacancy into a Mn ion occupying a Ga lattice site promotes a charge transfer from the Mn d band to the acceptor levels of V_{Ga} . Such a charge transfer lowers the

^{a)}Electronic mail: kchang@kaist.ac.kr

electronic energy, and hence the formation of a complex consisting of V_{Ga} and the Mn ion at a Ga site is energetically very stable. In addition, the Mn ion is strongly bonded to one of the neighboring N atoms around the V_{Ga} defect and electrically deactivates the dangling bond orbital of the corresponding N atom. Then, the remaining N dangling bond orbitals of V_{Ga} form a moderately shallow level. When a Ga vacancy interacts with two Mn ions, which are located at the percolation distance of about 6 Å in diluted Mn-doped GaN, we also find the depopulation of the Mn d band by the charge transfer from the Mn ions to the Ga vacancy. In this complex, two strong Mn–N bonds around the V_{Ga} defect broaden the Mn d band and reduce the density of states at the Fermi level. Thus, the ferromagnetic stability between the Mn ions is weakened because of the depopulation of the Mn d band and the chemical bonding effect. However, the ferromagnetism is still maintained due to the lack of antiferromagnetic superexchange interactions between the Mn ions at the percolation length, in contrast to the case of the nearest-neighbor distance.

II. CALCULATIONAL METHODS

Our calculations were performed within the density-functional-theory framework²⁶ in the spin-polarized generalized-gradient approximation (GGA),²⁷ using the PWSCF package.²⁸ Ultrasoft pseudopotentials²⁹ were employed for the efficient treatment of the localized orbitals. The wave functions were expanded in plane waves up to a cutoff of 30 Ry, which gives the accuracy of total energy differences to within a few tens of meV, as compared to a higher cutoff of 40 Ry. The ionic positions were fully relaxed using the conjugate gradient method. We chose a hexagonal supercell containing 72 atoms in the wurtzite structure. The Brillouin zone integration was done using the special \mathbf{k} -points generated by the $3 \times 3 \times 3$ Monkhorst-Pack mesh.³⁰ The GGA approach usually overestimates the position of the transition metal d states. To see the effect of strong electron-electron interactions on the electronic structure of defects, we carried out the GGA+ U calculations,³¹ in which the strong Coulomb repulsion U is taken into account for the localized Mn d electrons. In this case, we used the projector augmented wave (PAW) potentials,^{32,33} which are implemented in the VASP code.³⁴

III. RESULTS AND DISCUSSION

A. The electronic structure of the $\text{Mn}_{\text{Ga}}-V_{\text{Ga}}$ complex

We consider a $\text{Mn}_{\text{Ga}}-V_{\text{Ga}}$ complex which consists of a Ga vacancy (V_{Ga}) and a Mn ion (Mn_{Ga}) at a Ga sublattice site in the first neighborhood of V_{Ga} . Depending on the position of the Mn ion, three isomers exist in the $\text{Mn}_{\text{Ga}}-V_{\text{Ga}}$ complex, as shown in Figs. 1(a)–1(c). For all the isomers, the Mn ion is directly bonded to one of the N atoms around the V_{Ga} defect, which is denoted by N^* . It is known that an isolated Mn_{Ga} impurity forms the bonding t^b and antibonding t^a states, with the nonbonding e state lying between them near the valence band maximum (VBM). The antibonding t^a states are partially occupied [Fig. 2(a)], and the acceptor transition level $\epsilon(1-/0)$ lies deep in the band gap, in good

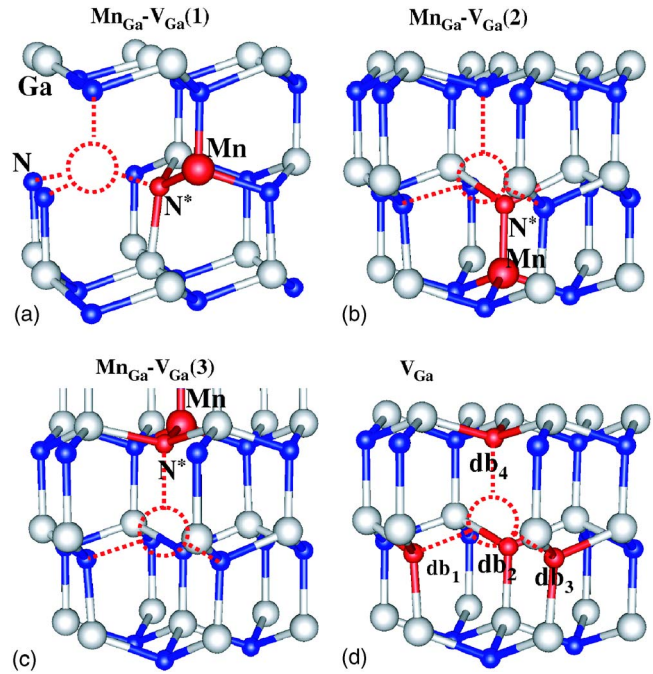


FIG. 1. (Color online) (a)–(c) The atomic structures for three isomers of the $\text{Mn}_{\text{Ga}}-V_{\text{Ga}}$ complex and (d) a Ga vacancy in wurtzite GaN. Dotted circles represent the position of the Ga vacancy, N^* is the N atom bonded to the Mn ion around the vacancy site, and db_i denotes the dangling bond orbitals.

agreement with experiments¹⁰ and previous theoretical calculations.^{11,25,35} Since the t^a states are higher than the acceptor levels of V_{Ga} , as shown in Fig. 2, a charge transfer of about 2 electrons occurs from the Mn ion to the Ga vacancy

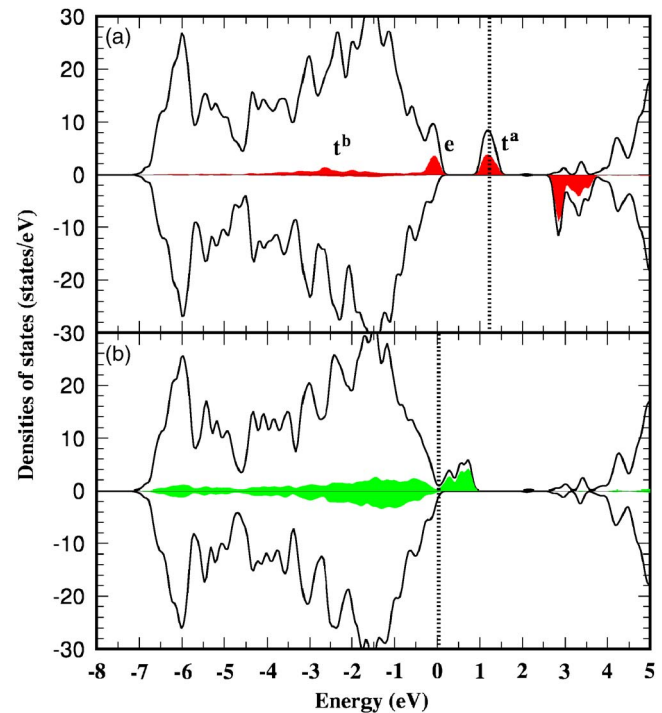


FIG. 2. (Color online) The total densities of states (solid lines) are compared for the (a) isolated Mn_{Ga} and (b) V_{Ga} defects. Red and green shaded areas represent the densities of states projected onto the Mn $3d$ and N $2p$ ions surrounding the Ga vacancy, respectively. The vertical dotted lines denote the Fermi level, with the VBM set to zero.

when the $\text{Mn}_{\text{Ga}}\text{-V}_{\text{Ga}}$ complex is formed. This charge transfer reduces the $\text{Mn}_{\text{Ga}}\text{-N}$ bond distances by 0.10–0.13 Å. In this case, the N^* atom adjacent to the Ga vacancy is more tightly bonded to the Mn ion, with the $\text{Mn}_{\text{Ga}}\text{-N}^*$ bond distance of 1.70 Å, which is smaller by 0.15 Å than the other three bonds.

The V_{Ga} defect has four dangling N bonds, which generate the acceptor levels in the band gap. Due to Hund's rule, a spin-polarized configuration is energetically more favorable for the Ga vacancy as long as the defect levels are not fully occupied by 3 electrons.²⁴ In the $\text{Mn}_{\text{Ga}}\text{-V}_{\text{Ga}}$ complex, the Ga vacancy, which is effectively in the 2- charge state due the charge transfer, carries a local spin moment of about 1 μ_B , while the Mn ion in the 5+ charge state has a local spin moment of about 2 μ_B . Between these two localized spin moments, we find that an antiferromagnetic spin configuration is more stable by 25 meV than a ferromagnetic one. In the antiferromagnetic spin state, the binding energy of the most stable $\text{Mn}_{\text{Ga}}\text{-V}_{\text{Ga}}(1)$ complex [see Fig. 1(a)] is calculated to be 2.60 eV with respect to individual neutral defects, while those for the other complexes, $\text{Mn}_{\text{Ga}}\text{-V}_{\text{Ga}}(2)$ and $\text{Mn}_{\text{Ga}}\text{-V}_{\text{Ga}}(3)$ in Figs. 1(b) and 1(c), are 2.54 and 2.47 eV, respectively. These large binding energies result from a release of strains accumulated around the lattice mismatched Mn ion and Coulomb attractive interactions between the two oppositely charged defects.

The electronic structure of the $\text{Mn}_{\text{Ga}}\text{-V}_{\text{Ga}}(2)$ complex is found to be similar to that of the $\text{Mn}_{\text{Ga}}\text{-V}_{\text{Ga}}(1)$ complex. Here, we compare the densities of states for the $\text{Mn}_{\text{Ga}}\text{-V}_{\text{Ga}}(1)$ and $\text{Mn}_{\text{Ga}}\text{-V}_{\text{Ga}}(3)$ complexes in Figs. 3(a) and 3(b). In the $\text{Mn}_{\text{Ga}}\text{-V}_{\text{Ga}}$ complex, both the Mn e and t' bands in minority spin states are significantly lowered, while those in majority spin states are not much affected, as compared to the isolated Mn_{Ga} defect. The lowering of the minority bands is attributed to the charge transfer of about 2 electrons from the Mn ion to the Ga vacancy, which results in the reduction of the exchange splitting between the Mn d levels. When the Mn_{Ga} ion is well separated by a distance of about 7.6 Å from the Ga vacancy, only the charge transfer from Mn_{Ga} to V_{Ga} occurs, leading to the lowering of the majority Mn t' band, as shown in Fig. 3(c). In this case, the Mn t' band is partially occupied; thus, the amount of transferred electrons is less than 2; from the analysis of the Mn 3d-projected density of states, the transferred charge is estimated to be about 1.4 electrons. In the $\text{Mn}_{\text{Ga}}\text{-V}_{\text{Ga}}$ complex, the Mn_{Ga} ion is strongly bonded to the N^* atom. Since the $\text{Mn}_{\text{Ga}}\text{-N}^*$ bond raises the majority Mn t' band with the antibonding characteristics, this band remains almost unchanged.

In the $\text{Mn}_{\text{Ga}}\text{-V}_{\text{Ga}}$ complex, since V_{Ga} is effectively in the 2- charge state due to the charge transfer, we compare the (1-/0) transition level of the complex with the (3-/2-) level of an isolated V_{Ga} . In the isolated V_{Ga} defect, the (3-/2-) transition level is associated with interactions between the dangling bond orbitals of the neighboring N atoms, and this level lies deep in the band gap due to the crystal-field effect. Using a 108-atom supercell, we find that the isolated V_{Ga} defect has the (3-/2-) transition level at 1.03 eV above the VBM.³⁶ For the $\text{Mn}_{\text{Ga}}\text{-V}_{\text{Ga}}(1)$ complex, the (1-/0) transition level is lowered to 0.52 eV above the

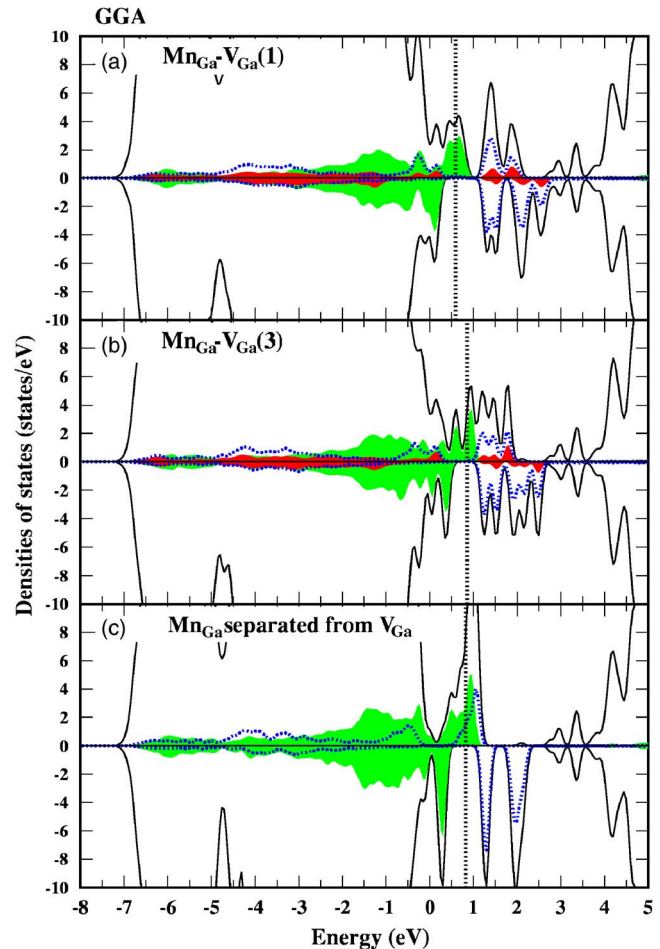


FIG. 3. (Color online) The total (solid lines) and Mn 3d-projected (blue dotted lines) densities of states obtained from the GGA calculations are compared for the (a) $\text{Mn}_{\text{Ga}}\text{-V}_{\text{Ga}}(1)$ and (b) $\text{Mn}_{\text{Ga}}\text{-V}_{\text{Ga}}(3)$ complexes in Fig. 1, and (c) the Mn_{Ga} defect separated by 7.6 Å from V_{Ga} . In (a) and (b), red and green shaded areas represent the densities of states projected onto the N^* and other N atoms surrounding the Ga vacancy, respectively, while in (c) green shaded area represents the density of states projected onto all the N atoms around V_{Ga} . The vertical dotted lines denote the Fermi level, with the VBM set to zero.

VBM. As mentioned earlier, the N^* atom in the neighborhood of V_{Ga} interacts more strongly with the Mn_{Ga} ion than the other N atoms only bonded to the three Ga atoms. The strong $\text{Mn}_{\text{Ga}}\text{-N}^*$ bond lowers the dangling bond state associated with the N^* atom into the valence band, while the other dangling bond states remain right above the VBM, as illustrated in Figs. 3(a) and 3(b). The N^* dangling bond orbital is fully occupied, passivated by the transferred charge from the Mn_{Ga} ion, and hence almost decoupled from the other dangling bond orbits. The three remaining dangling bond orbits interact less strongly with each other, compared with those for the isolated V_{Ga} , resulting in a shallower acceptor level. Although V_{Ga} has four dangling bond orbitals [see Fig. 1(d)], the characteristics of the db_4 orbital lying along the hexagonal axis is different from the others, db_1 , db_2 , and db_3 , due to the wurtzite symmetry. When a dangling bond orbital is passivated by the Mn_{Ga} ion, the acceptor level and the Fermi level of the neutral $\text{Mn}_{\text{Ga}}\text{-V}_{\text{Ga}}$ complex vary with the type of the dangling bond. In the $\text{Mn}_{\text{Ga}}\text{-V}_{\text{Ga}}(1)$ complex, where the db_1 orbital is electrically deactivated, the Fermi

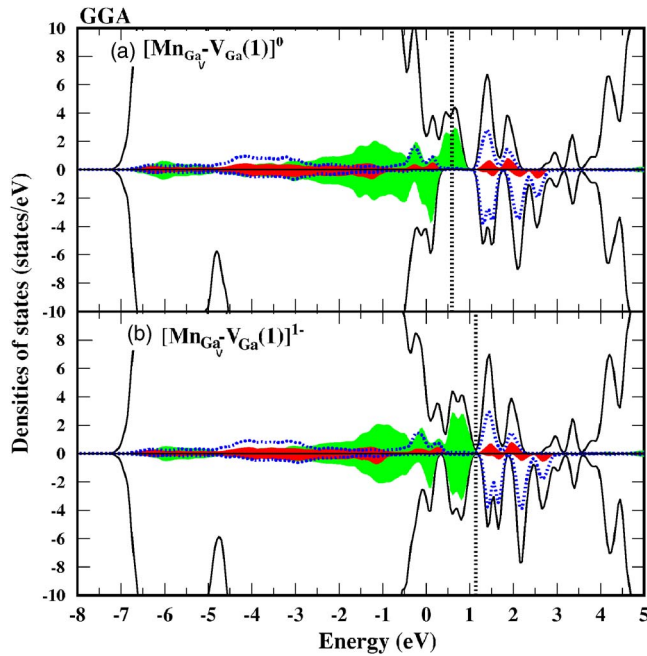


FIG. 4. (Color online) The total (solid lines) and Mn 3d-projected (blue dotted lines) densities of states obtained from the GGA calculations are compared for the $\text{Mn}_{\text{Ga}}\text{-V}_{\text{Ga}}(1)$ complex in the (a) neutral and (b) 1- charge states. Red and green shaded areas represent the densities of states projected onto the N^* and other N atoms surrounding the Ga vacancy, respectively. The vertical dotted lines denote the Fermi level, with the VBM set to zero.

level is positioned at 0.59 eV above the VBM, while a higher Fermi level of 0.86 eV is found for the $\text{Mn}_{\text{Ga}}\text{-V}_{\text{Ga}}(3)$ complex with the db_4 orbital passivated.

To see the effect of the deactivation of the N dangling bond orbital on the acceptor level, we examine the electronic structure of $(\text{V}_{\text{Ga}}\text{-H})^{1-}$, in which V_{Ga} is effectively in the 2- charge state with one of its dangling bond orbitals passivated by hydrogen. Recently, the $\text{V}_{\text{Ga}}\text{-H}$ complex was experimentally identified in GaN epitaxially grown by metalorganic chemical-vapor deposition.³⁷ When the db_1 orbital is passivated by H, the Fermi level of $(\text{V}_{\text{Ga}}\text{-H})^{1-}$ lies at 0.54 eV above the VBM, which is lower by 0.31 eV than that for the $\text{V}_{\text{Ga}}^{2-}$ defect. If V_{Ga} is passivated by 2 H atoms, the Fermi level of the $(\text{V}_{\text{Ga}}\text{-2H})^0$ defect is further reduced to 0.12 eV. For the $(\text{V}_{\text{Ga}}\text{-H})^{1-}$ defect, with the db_4 orbital passivated by 1 H atom, the Fermi level is located at a higher energy of 0.74 eV above the VBM. Our results indicate that the lowering of the acceptor level in the $\text{Mn}_{\text{Ga}}\text{-V}_{\text{Ga}}$ complex is caused by the weaker coupling between the remaining dangling bond orbitals, as compared to the isolated V_{Ga} defect.

Based on our calculations for the $\text{Mn}_{\text{Ga}}\text{-V}_{\text{Ga}}$ and $\text{V}_{\text{Ga}}\text{-H}$ complexes, we can understand the shallowness of the acceptor level of the $\text{As}_{\text{Zn}}\text{-2V}_{\text{Zn}}$ complex, which was suggested to be the origin of the p -type conductivity in As-doped ZnO.³⁸ In the $\text{As}_{\text{Zn}}\text{-2V}_{\text{Zn}}$ complex, one of the neighboring O atoms around each Zn vacancy is bonded to the As_{Zn} ion, and the corresponding dangling bond orbital is electrically deactivated. Then, the remaining active dangling bond orbitals lead to the shallower acceptor level than for the V_{Zn} defect.

Next, we perform the GGA+ U calculations³¹ to investigate the effect of strong electron-electron interactions on the electronic structure of the $\text{Mn}_{\text{Ga}}\text{-V}_{\text{Ga}}$ complex. The on-site

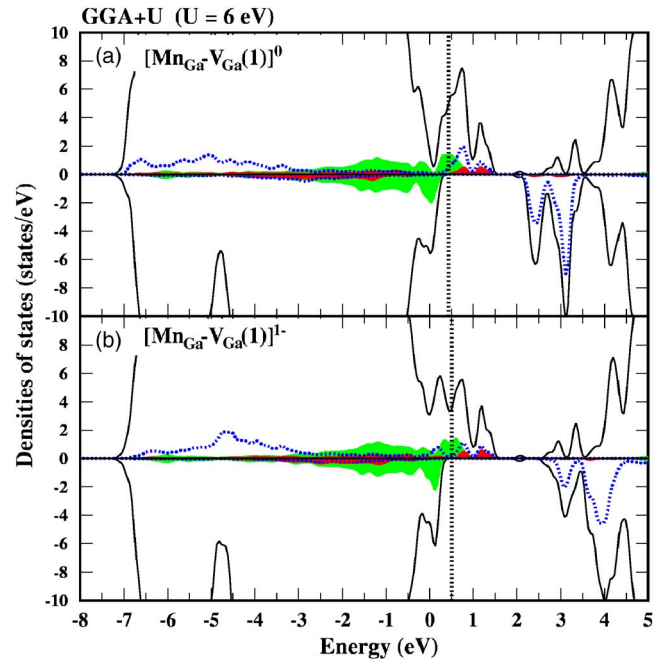


FIG. 5. (Color online) The total (solid lines) and Mn 3d-projected (blue dotted lines) densities of states from the GGA+ U calculations with $U = 6$ eV are compared for the $\text{Mn}_{\text{Ga}}\text{-V}_{\text{Ga}}(1)$ complex in the (a) neutral and (b) 1- charge states. Red and green shaded areas represent the densities of states projected onto the N^* and other N atoms surrounding the Ga vacancy, respectively. The vertical dotted lines denote the Fermi level, with the VBM set to zero.

Coulomb interaction parameter U of the Mn d orbitals is varied from 4 to 6 eV, and the exchange parameter J is chosen to be 1 eV, which was widely used in previous calculations.^{39,40} For an isolated neutral Mn_{Ga} defect, as the parameter U increases, the partially occupied Mn t^a band in majority spin states is lowered toward the valence band and lies just above the VBM with the Fermi level of 0.36 eV for $U=6$ eV, while the unoccupied Mn d bands in minority spin states move to higher energies. The GGA densities of states (Fig. 4) of the $\text{Mn}_{\text{Ga}}\text{-V}_{\text{Ga}}$ complex are compared with those (Fig. 5) obtained from the GGA+ U calculations. In the neutral $\text{Mn}_{\text{Ga}}\text{-V}_{\text{Ga}}$ complex, the GGA+ U calculations show that the empty t^a band in majority spin states shifts to the valence band as U increases. For $U=6$ eV, the majority Mn t^a band is positioned just above the Fermi level and still empty, as shown in Fig. 5(a). The positions and occupancies of the defect levels of V_{Ga} are not affected in the GGA+ U calculations, with similar Fermi levels of about 0.5 eV above the VBM.

When the $\text{Mn}_{\text{Ga}}\text{-V}_{\text{Ga}}$ complex is in the 1- charge state, however, we find a large change in the density of states, as shown in Fig. 5(b). As U increases from 0 to 6 eV, the majority Mn t^a band is significantly lowered toward the valence band, being partially occupied by the doped electron. In fact, for $U=5$ or 6 eV, we find that the charge state of the Mn ion changes from 5+ to 4+ when an electron is doped in the $\text{Mn}_{\text{Ga}}\text{-V}_{\text{Ga}}$ complex (see Table I). In addition, since the Fermi level of the $(\text{Mn}_{\text{Ga}}\text{-V}_{\text{Ga}})^{1-}$ complex decreases from 1.14 to 0.50 eV, the stability of this complex is enhanced. Therefore, the (1- / 0) transition level of the $\text{Mn}_{\text{Ga}}\text{-V}_{\text{Ga}}$ complex decreases as the parameter U increases; for $U=6$ eV,

TABLE I. The charge states of the Mn ion and the Ga vacancy in the isolated Mn_{Ga} defect and the $(\text{Mn}_{\text{Ga}}-V_{\text{Ga}})^q$ complex are compared for various values of the on-site Coulomb interaction parameter U , where q is the charge state of the complex.

	$(\text{Mn}_{\text{Ga}})^0$	$(\text{Mn}_{\text{Ga}}-V_{\text{Ga}})^0$	$(\text{Mn}_{\text{Ga}}-V_{\text{Ga}})^{1-}$
$U=0, 4 \text{ eV}$	Mn^{3+}	$\text{Mn}^{5+}, V_{\text{Ga}}^{2-}$	$\text{Mn}^{5+}, V_{\text{Ga}}^{2-}$
$U=5, 6 \text{ eV}$	Mn^{3+}	$\text{Mn}^{5+}, V_{\text{Ga}}^{2-}$	$\text{Mn}^{4+}, V_{\text{Ga}}^{2-}$

we estimate the $(1-/0)$ transition level to be about 0.25 eV above the VBM, which is shallower by 0.27 eV than the value obtained from the GGA calculations. The shallowness of this acceptor level may explain the p -type conductivity observed in GaMnN thin films deposited on periodically Mn δ -doped GaN buffer layers grown by using a rf-assisted molecular beam epitaxy with an active N_2 plasma source.^{22,41}

B. The effect of Ga vacancy on the magnetic properties of Mn-doped GaN

Recently, Mahadevan and co-workers²⁴ studied the effect of the presence of V_{Ga} on the magnetic interactions between two Mn ions, which are placed at the nearest-neighbor Ga sites. For various positions of V_{Ga} , they found that the depopulation of the Mn d band by the acceptor levels of V_{Ga} results in a reduction of the exchange splitting in the Mn d levels, and hence it destroys ferromagnetism. When ferromagnetic interactions are weakened by the depopulation of the Mn d band, antiferromagnetic superexchange interactions play a role in destabilizing the ferromagnetic state, especially for the Mn ions located at the nearest-neighbor distance. In other calculations, ferromagnetic interactions were shown to be strongest for the Mn ions at the nearest-neighbor distance and decay rapidly as the Mn-Mn distance increases, with the short-range nature.^{11,15,16,25} However, in diluted Mn-doped GaN, it is more appropriate to consider the Mn ions separated by a percolation length in determining the Curie temperature, while the Curie temperature strongly depends on the nearest-neighbor coupling in the mean-field approximation.^{15,16} In our study, we choose two Mn ions, Mn_{I} and Mn_{II} , which are positioned at the origin and the (1, 1, 1) site in terms of the primitive lattice vectors in the wurtzite structure. The distance between the two Mn ions is about 6 Å, close to the percolation-threshold length estimated from a three-dimensional random-site model for the Mn concentration of 6%.^{25,42} For the $\text{Mn}_{\text{I}}-\text{Mn}_{\text{II}}$ complex, we find that the ferromagnetic state is more stable by about 105 meV than the antiferromagnetic spin configuration.

We consider a $\text{Mn}_{\text{I}}-V_{\text{Ga}}-\text{Mn}_{\text{II}}$ complex [see Fig. 6(a)], where a Ga vacancy is located between the two Mn ions, and examine the role of V_{Ga} on ferromagnetism, focusing on the charge transfer and chemical bonding effects. The binding energy of this complex is calculated to be 3.6 eV with respect to well-separated V_{Ga} and $\text{Mn}_{\text{I}}-\text{Mn}_{\text{II}}$. Similar to the $\text{Mn}_{\text{Ga}}-V_{\text{Ga}}$ complex, we find a charge transfer of 3 electrons from the majority Mn t^a band to the acceptor levels of V_{Ga} . Thus, the defect levels of V_{Ga} are fully occupied and spin-nonpolarized. In the $\text{Mn}_{\text{Ga}}-\text{Mn}_{\text{Ga}}$ pair, the exchange splitting of the Mn d levels tends to decrease by hole doping,

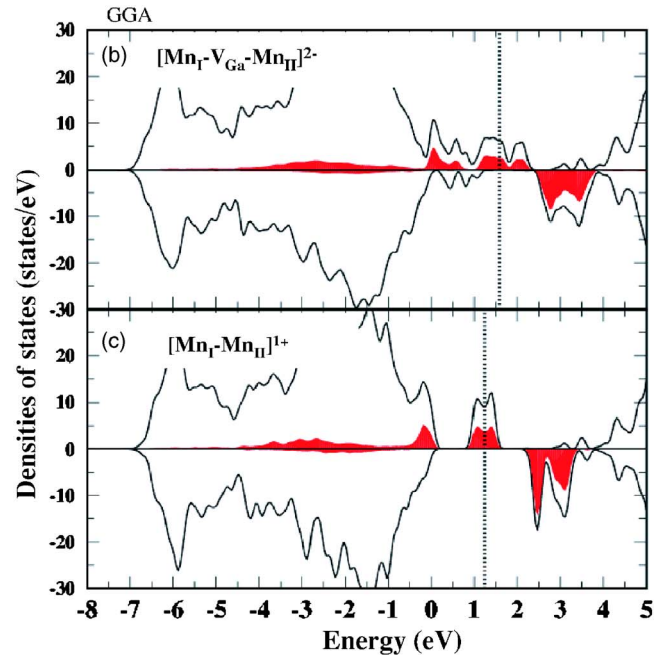
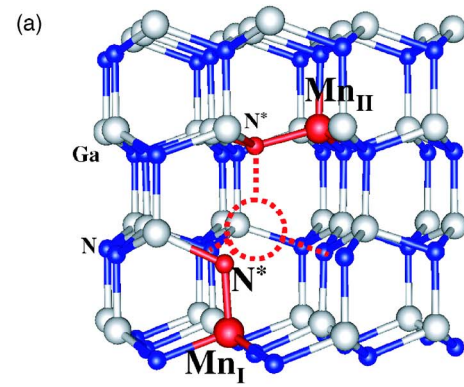


FIG. 6. (Color online) (a) The atomic structure of the $\text{Mn}_{\text{I}}-V_{\text{Ga}}-\text{Mn}_{\text{II}}$ complex, where V_{Ga} (denoted as a dotted circle) is positioned between the two Mn ions, which are located at the origin and the (1, 1, 1) site in terms of the primitive lattice vectors of wurtzite GaN. The total (solid lines) and Mn 3d-projected (red shaded areas) densities of states obtained from the GGA calculations are compared for the (b) $(\text{Mn}_{\text{I}}-V_{\text{Ga}}-\text{Mn}_{\text{II}})^{2-}$ and (c) $(\text{Mn}_{\text{I}}-\text{Mn}_{\text{II}})^{1+}$ complexes. The vertical dotted lines denote the Fermi level, with the VBM set to zero.

whereas it increases by electron doping.²⁵ Since the depopulation of the Mn t^a band is equivalent to the hole-doped case, the exchange splitting is found to decrease from 2 to 1 eV by the presence of V_{Ga} . The decrease of the exchange splitting will reduce the stability of the ferromagnetic state. For the Mn-Mn distance of 6 Å considered here, the antiferromagnetic superexchange interaction is much weakened; the number of electrons that contribute to the superexchange interaction decreases from 2 to 0.5 electrons/Mn by the charge transfer effect. Thus, although the decrease of the exchange splitting reduces the stability of the ferromagnetic state, we find that the ferromagnetic state is still more favorable by about 15 meV than the antiferromagnetic spin state, in contrast to the previous calculational results for the Mn-Mn pair at the nearest-neighbor distance.²⁴

In the $\text{Mn}_{\text{I}}-V_{\text{Ga}}-\text{Mn}_{\text{II}}$ complex, two strong Mn-N* bonds are formed, as shown in Fig. 6(a). To see the effect of

TABLE II. The total energies (ΔE in units of meV) of the ferromagnetic state relative to the antiferromagnetic spin configuration are compared for the (Mn-Mn) q and (Mn- V_{Ga} -Mn) q complexes for various charge states (q), with the two Mn ions positioned at the percolation distance of about 6 Å in Fig. 6(a). Here, n_e (in units of electrons per Mn) denotes the number of electrons populated in the Mn t^a band.

n_e	ΔE for (Mn-Mn) q	ΔE for (Mn- V_{Ga} -Mn) q
2.0	-104.8($q=0$)	-8.8($q=-3$)
1.5	-143.2($q=+1$)	-40.7($q=-2$)
0.5	-53.3($q=+3$)	-15.0($q=0$)

the Mn-N * bonds on the ferromagnetism, we compare the total energies of the (Mn $_I$ -Mn $_{II}$) q and (Mn $_I$ - V_{Ga} -Mn $_{II}$) $^{q'}$ complexes, with the same populations of the Mn t^a band, where q and q' denote charge states, and $q'=q-3$ due to the charge transfer effect. The total energies (ΔE) of the ferromagnetic state relative to the antiferromagnetic spin configuration are listed for various charge states in Table II. For both the Mn-Mn pairs with and without the Ga vacancy, the ferromagnetic stability is enhanced as the number of populated electrons (n_e) in the Mn d band decreases from 2.0 to 1.5 e/Mn , and then it decreases for $n_e=0.5e/\text{Mn}$, in consistency with the previously calculated results.²⁵ For a given population of the Mn d band, the presence of V_{Ga} tends to weaken the stability of the ferromagnetic state; ΔE is reduced by 96.0, 102.5, and 38.3 meV for $n_e=2.0$, 1.5, and 0.5 e/Mn , respectively. Figures 6(b) and 6(c) show the densities of states for the Mn-Mn complex with $q=+1$ and the Mn- V_{Ga} -Mn complex with $q'=-2$. With the presence of V_{Ga} , the Fermi level lying in the Mn t^a band increases from 1.24 to 1.59 eV above the VBM, with the reduced density of states at the Fermi level. In addition, the majority Mn t^a band is much broadened with a large splitting due to the strong Mn-N * bonds. Thus, the number of carriers that contribute to spin-conserving hopping interactions between the Mn ions is reduced in the Mn- V_{Ga} -Mn complex. Since the ferromagnetic interaction is mediated by holes in the Mn d band, the reduction of hole carriers induced by the chemical bonding effect leads to the reduced ferromagnetic stability.

IV. SUMMARY

We have studied the interactions of V_{Ga} with the Mn ions and the role of V_{Ga} in modifying the defect and magnetic properties of Mn-doped GaN through the GGA and GGA+ U calculations. We find that the Mn- V_{Ga} complex, in which the Mn ion substitutes for a Ga site rather than a N site, is energetically very stable and behaves as a moderately shallow acceptor. In the GGA calculations, the acceptor transition level of the Mn- V_{Ga} complex is estimated to be 0.52 eV, while it decreases to 0.25 eV in the GGA+ U . The shallowness of the acceptor level is attributed to the charge transfer from the Mn d band to the acceptor levels of V_{Ga} and the strong Mn-N bond which electrically deactivates one of the dangling bond orbitals around the V_{Ga} defect. In the Mn- V_{Ga} -Mn complex, where the Mn ions are separated by the percolation distance of about 6 Å, we also find the charge transfer from the Mn ions to the V_{Ga} defect, which

reduces the exchange splitting of the Mn d levels. In addition, the formation of two strong Mn-N bonds leads to the broadening of the Mn d band and the reduction of the density of states at the Fermi level. Although both the charge transfer and chemical bonding effects weaken the ferromagnetic stability between the Mn ions at the percolation distance, the ferromagnetic state is still maintained with low Curie temperatures.

ACKNOWLEDGMENTS

This work was supported by the Star-Faculty Project (Grant No. KRF-2005-084-C00007), the Korea Ministry of Commerce, Industry, and Energy, and the QSRC at Dongguk University.

- ¹T. Dietl, H. Ohno, F. Matsukura, J. Cibert, and D. Ferrand, *Science* **287**, 1019 (2000).
- ²M. E. Overberg, C. R. Abernathy, S. J. Pearton, N. A. Theodoropoulou, K. T. McCarthy, and A. F. Hebard, *Appl. Phys. Lett.* **79**, 1312 (2001).
- ³M. L. Reed, N. A. El-Masry, H. H. Stadelmaier, M. K. Ritums, M. J. Reed, C. A. Parker, J. C. Roberts, and S. M. Bedaire, *Appl. Phys. Lett.* **79**, 3473 (2001).
- ⁴G. T. Thaler, M. E. Overberg, B. Gila, R. Frazier, C. R. Abernathy, S. J. Pearton, J. S. Lee, S. Y. Lee, Y. D. Park, Z. G. Khim, J. Kim, and F. Ren, *Appl. Phys. Lett.* **80**, 3964 (2002).
- ⁵N. Theodoropoulou, A. F. Hebard, M. E. Overberg, C. R. Abernathy, S. J. Pearton, S. N. G. Chu, and R. G. Wilson, *Appl. Phys. Lett.* **78**, 3475 (2001).
- ⁶T. Sasaki, S. Sonoda, Y. Yamamoto, K. Suga, S. Shimizu, K. Kindo, and H. Hori, *J. Appl. Phys.* **91**, 7911 (2002).
- ⁷K. H. Kim, K. J. Lee, D. J. Kim, H. J. Kim, Y. E. Ihm, C. G. Kim, S. H. Yoo, and C. S. Kim, *Appl. Phys. Lett.* **82**, 4755 (2003).
- ⁸S. Dhar, O. Brandt, A. Trampert, K. J. Friedland, Y. J. Sun, and K. H. Ploog, *Phys. Rev. B* **67**, 165205 (2003).
- ⁹R. Y. Korotkov, J. M. Gregie, and B. W. Wessels, *Appl. Phys. Lett.* **80**, 1731 (2002).
- ¹⁰T. Graf, M. Gjukic, M. S. Brandt, M. Stutzmann, and O. Ambacher, *Appl. Phys. Lett.* **81**, 5159 (2002).
- ¹¹P. Mahadevan and A. Zunger, *Appl. Phys. Lett.* **85**, 2860 (2004).
- ¹²T. Graf, S. T. B. Goennenwein, and M. S. Brandt, *Phys. Status Solidi B* **239**, 277 (2003).
- ¹³H. Akai, *Phys. Rev. Lett.* **81**, 3002 (1998).
- ¹⁴K. Sato, P. H. Dederichs, and H. Katayama-Yoshida, *Europhys. Lett.* **61**, 403 (2003).
- ¹⁵K. Sato, W. Schweika, P.H. Dederichs, and H. Katayama-Yoshida, *Phys. Rev. B* **70**, 201202(R) (2004).
- ¹⁶L. Bergqvist, O. Eriksson, J. Kudrnovský, V. Drchal, P. Korzhavyi, and I. Turek, *Phys. Rev. Lett.* **93**, 137202 (2004).
- ¹⁷K. Sato, H. Katayama-Yoshida, and P. H. Dederichs, *Jpn. J. Appl. Phys., Part 2* **44**, L948 (2005).
- ¹⁸T. Fukushima, K. Sato, H. Katayama-Yoshida, and P. H. Dederichs, *Jpn. J. Appl. Phys., Part 2* **45**, L416 (2006).
- ¹⁹H. Katayama-Yoshida, K. Sato, T. Fukushima, M. Toyoda, H. Kizaki, V. A. Dinh, and P. H. Dederichs, *Phys. Status Solidi A* **204**, 15 (2007).
- ²⁰K. Sato, T. Fukushima, and H. Katayama-Yoshida, *Jpn. J. Appl. Phys., Part 2* **46**, L682 (2007).
- ²¹H. Munekata, H. Ohno, S. von Molnar, A. Segmüller, L. L. Chang, and L. Esaki, *Phys. Rev. Lett.* **63**, 1849 (1989).
- ²²H. C. Jeon, T. W. Kang, T. W. Kim, J. Kang, and K. J. Chang, *Appl. Phys. Lett.* **87**, 092501 (2005).
- ²³E. J. Tarsa, B. Heying, X. H. Wu, P. Fini, S. P. DenBaars, and J. S. Speck, *J. Appl. Phys.* **82**, 5472 (1997).
- ²⁴P. Mahadevan and S. Mahalakshmi, *Phys. Rev. B* **73**, 153201 (2006).
- ²⁵J. Kang, K. J. Chang, and H. Katayama-Yoshida, *J. Supercond.* **18**, 55 (2005).
- ²⁶P. Hohenberg and W. Kohn, *Phys. Rev.* **136**, B864 (1964); W. Kohn and L. J. Sham, *ibid.* **140**, A1133 (1965).
- ²⁷J. P. Perdew, in *Electronic Structure of Solids*, edited by P. Ziesche and H.

- Eschrig (Akademie-Verlag, Berlin, 1991).
- ²⁸S. Baroni, A. Dal Corso, D. de Gironcoli, and P. Giannozzi, <http://www.pwscf.org>
- ²⁹D. Vanderbilt, Phys. Rev. B **41**, 7892 (1990).
- ³⁰H. J. Monkhorst and J. D. Pack, Phys. Rev. B **13**, 5188 (1976).
- ³¹A. I. Liechtenstein, V. I. Anisimov, and J. Zaanen, Phys. Rev. B **52**, R5467 (1995).
- ³²P. E. Blöchl, Phys. Rev. B **50**, 17953 (1994).
- ³³G. Kresse and D. Joubert, Phys. Rev. B **59**, 1758 (1999).
- ³⁴G. Kresse and J. Furthmüller, Phys. Rev. B **54**, 11169 (1996).
- ³⁵P. Mahadevan and A. Zunger, Phys. Rev. B **68**, 075202 (2003).
- ³⁶The errors in the total energy and the Fermi level caused by the use of the jellium background charge are large for multiply charged defects such as V_{Ga}^{2-} and V_{Ga}^{3-} in small-sized supercells. For the Ga vacancy, we obtain the $(3-/2-)$ transition levels at 0.74 and 1.03 eV using the 72- and 108-atom supercells, respectively. Here, we use the 108-atom supercell to compare the Fermi level and the acceptor levels of the multiply charged Ga vacancy with those for the $\text{Mn}_{\text{Ga}}-V_{\text{Ga}}$ complex.
- ³⁷S. Hautakangas, I. Makkonen, V. Ranki, M. J. Puska, K. Saarinen, X. Xu, and D. C. Look, Phys. Rev. B **73**, 193301 (2006).
- ³⁸S. Limpijumnong, S. B. Zhang, S.-H. Wei, and C. H. Park, Phys. Rev. Lett. **92**, 155504 (2004).
- ³⁹B. Sanyal, O. Bengone, and S. Mirbt, Phys. Rev. B **68**, 205210 (2003).
- ⁴⁰M. Wierzbowska, D. Sánchez-Portal, and S. Sanvito, Phys. Rev. B **70**, 235209 (2004).
- ⁴¹Since periodically Mn δ -doped layers induce large strains in the GaN region, abundant Ga vacancies would be promoted near the Mn layers, forming the $\text{Mn}_{\text{Ga}}-V_{\text{Ga}}$ complexes during epitaxial growth under N-rich conditions, although the formation energy of V_{Ga} is known to be high, especially in p -type GaN [C. G. Van de Walle and J. Neugebauer, J. Appl. Phys. **95**, 3851 (2004)].
- ⁴²D. F. Holcomb and J. J. Rehr, Jr., Phys. Rev. **183**, 773 (1969).